

**INCREASING THE STRENGTH OF ADHESIVELY  
BONDED JOINTS BY TAPERING THE ADHERENDS**

K. E. Metzinger and T. R. Guess  
Sandia National Laboratories  
Albuquerque, New Mexico

RECEIVED  
OCT 28 1999  
ST

**ABSTRACT**

Wind turbine blades are often fabricated with composite materials. These composite blades are frequently attached to a metallic structure with an adhesive bond. For the baseline composite-to-steel joint considered in this study, failure typically occurs when the adhesive debonds from the steel adherend. Previous efforts established that the adhesive peel stresses strongly influence the strength of these joints for both single-cycle and fatigue loading. This study focused on reducing the adhesive peel stresses present in these joints by tapering the steel adherends. Several different tapers were evaluated using finite element analysis before arriving at a final design. To confirm that the selected taper was an improvement to the existing design, the baseline joint and the modified joint were tested in both compression and tension. In these axial tests, the compressive strengths of the joints with tapered adherends were greater than those of the baseline joints for both single-cycle and low-cycle fatigue. In addition, only a minor reduction in tensile strength was observed for the joints with tapered adherends when compared to the baseline joints. Thus, the modification would be expected to enhance the overall performance of this joint.

**INTRODUCTION**

When adhesively bonded lap joints are utilized as blade attachments in a wind turbine, the satisfactory performance of these joints is critical to the viability of the turbine. In order to improve the durability of these joints, several test series and analyses have been conducted. Previous efforts<sup>1,2</sup> established that the adhesive peel stresses strongly affect the performance of the baseline joint considered in this study for both single-cycle and fatigue loading. (A similar study<sup>3</sup> involving joints with a much thinner adhesive layer showed the same effect.) In these earlier tests, the baseline geometry was subjected to compressive and tensile loading. Compressive and tensile loads of

the same magnitude produce adhesive stresses and strains with very similar magnitudes. However, for the joint considered, tensile loads produce compressive peel stresses in the adhesive where debonding initiates while compressive loads produce tensile peel stresses at this location. The joints were shown to be significantly stronger in tension than compression for both single-cycle and low-cycle fatigue axial loading. In addition, adhesive debonding was only observed on the compressive sides of the bending specimens which were tested in high-cycle fatigue. These clear differences established the importance of the localized peel (normal) stresses that develop in the adhesive at the steel adherend interface. They also established that the limiting factor for these joints is their response to compressive loading. Thus, the compressive strength of these joints must be increased in order to improve their overall performance.

In this study, several different tapers to the steel adherend were evaluated using finite element analysis. Modified joints (fabricated with the selected taper) were then tested along with joints with a uniform steel adherend (baseline design). These axial tests revealed that the performance of the modified joints under compressive loading was superior to joints of the baseline design. In addition, the modified joints were nearly as strong under tensile loading as the baseline joints. Since the baseline design joints are much weaker in compression than tension, this modification enhances their overall performance. It should be noted that other modifications could also enhance the performance of this joint. The selected taper is intended to demonstrate the feasibility of improving the performance of this joint. It is not the result of an exhaustive optimization effort.

Figure 1 shows the geometries of the baseline tensile and compressive specimens. The dimensions of the tapered steel adherend used for the compressive specimens are shown in Figure 2. The tapered steel adherends used for the tensile

## **DISCLAIMER**

**This report was prepared as an account of work sponsored by an agency of the United States Government. Neither the United States Government nor any agency thereof, nor any of their employees, make any warranty, express or implied, or assumes any legal liability or responsibility for the accuracy, completeness, or usefulness of any information, apparatus, product, or process disclosed, or represents that its use would not infringe privately owned rights. Reference herein to any specific commercial product, process, or service by trade name, trademark, manufacturer, or otherwise does not necessarily constitute or imply its endorsement, recommendation, or favoring by the United States Government or any agency thereof. The views and opinions of authors expressed herein do not necessarily state or reflect those of the United States Government or any agency thereof.**

## **DISCLAIMER**

**Portions of this document may be illegible in electronic image products. Images are produced from the best available original document.**

specimens have the same dimensions as those used for the compressive specimens, with one exception. The 0.275-inch thick portion of the adherends is two inches longer in order to accommodate the internal threads at their open ends. Note that the tapered steel adherend is quite thin (0.05 inches) at one end. Indeed, a finite element analysis indicated that the tapered steel adherends would yield prior to joint failure if fabricated from a 1020 steel (as had been done in earlier studies involving only the baseline adherends). To keep the response of the steel adherends in the elastic regime, both the baseline and tapered steel adherends were fabricated from a higher strength (4130) steel for this study. In the single-cycle tests, the specimens were loaded until either the adhesive bond or the composite adherend completely failed. However, the low-cycle fatigue tests were terminated when the adhesive was determined - using ultrasonic inspection - to have partially debonded from either adherend.

## ANALYSES

### Finite Element Models

Figure 3 shows the axisymmetric finite element mesh used to model the baseline compressive specimens. The adhesive layer has sixteen elements through its thickness. The finite element mesh (see Figure 4) used to represent the modified compressive specimens utilizes the same discretization for the adhesive and the composite adherend as the baseline mesh. Both meshes are comprised of eight-node biquadratic, reduced integration, axisymmetric solid elements (CAX8R). All of the analyses - which allow for plastic deformations in the adhesive - were performed with ABAQUS<sup>4</sup>. Nonlinear geometric effects were included for completeness. The isotropic material properties used for the Hysol EA-9394 adhesive<sup>5</sup> and the 4130 steel<sup>6</sup> are listed in Table 1. The adhesive properties correspond to a high strength, room-temperature curing paste adhesive. The orthotropic material properties<sup>7</sup> listed in Table 2 represent a plain weave E-glass fabric/epoxy composite. The subscripts  $r$ ,  $a$ , and  $t$  in Table 2 refer to the radial, axial, and tangential directions, respectively.

It should be noted that several different tapers were evaluated using finite element analyses before selecting the one considered in this study. Although the primary objective was to reduce the adhesive

peel stresses at the location where debonding initiates in the baseline design, other factors were considered. To control costs, the modified steel tapers needed to be easily machined from readily available tubing. In addition, the small flat at the thin end of the adherend was necessary to accommodate the fabrication technique previously established for the baseline design.

### Results

Figure 5 shows the peel (normal) stresses that develop in the adhesive at the steel adherend interface for both the baseline and modified compressive specimens. The applied load of 40000 pounds represents a typical single-cycle failure value for the baseline design. Although the calculated values are dependent upon the corresponding finite element meshes, identical discretizations were used for the adhesive and the composite adherend and comparable discretizations were used for the baseline and tapered steel adherends. The end of the bond where failure initiates (the right end in Figures 3 and 4) corresponds to an axial bond location of 3 inches. Note that tapering the steel adherend reduces the high tensile peel stresses that develop in this region.

Although previous efforts<sup>1,2</sup> have established the deleterious effect of tensile peel stresses at this location, debonding has been observed in this region when the peel stresses were compressive (for tensile loading). Thus, the magnitude of the adhesive strains that develop in this region should also be considered. Figure 6 shows the plastic strains that develop in the adhesive at the steel adherend interface for a compressive load of 40000 pounds. Note that the equivalent plastic strains are not as localized as the peel stresses since they include the effects of the shear stresses as well. As shown in Figure 6, tapering the steel adherend also reduces the adhesive strains at the location where debonding is expected. Thus, it is anticipated that this modification will improve the compressive strength of these joints. However, testing will be required to establish and quantify any improvement.

Although tapering the steel adherend may increase the compressive strength of these joints, it could also reduce their tensile strength. (A small reduction would be acceptable since the joints are much stronger in tension than compression and

adhesive debonding always initiates on the compressive side in bending specimens.) When these joints are subjected to a tensile load of 40000 pounds, the magnitude of the adhesive stresses and strains will be very similar to those shown in Figures 5 and 6. However, the sign of the peel stresses will be reversed. While the reduction in the adhesive plastic strains is desirable, the reduction in the compressive peel stresses may not be. The net result of these presumably competing effects is unclear, but will be addressed with testing.

A final concern is whether the selected modification might lead to adhesive debonding at the composite adherend interface. Figures 7 and 8 show the adhesive peel stresses and plastic strains that develop at the composite adherend interface for a compressive load of 40000 pounds. It is difficult to assess whether the change in the adhesive plastic strains is beneficial or detrimental since the modification increases the plastic strain at the extreme end of the bond, but lowers it elsewhere. The interpretation of the peel stresses is more straightforward. For a compressive load, tapering the adherend increases the compressive peel stresses and should not be a problem. However, for a tensile load, the modified joints will develop higher tensile peel stresses and could lead to debonding at this interface. Once again, testing will be required to determine if this occurs.

## EXPERIMENTS

### Specimen Fabrication

Prior to fabrication, the composite and steel adherends were lightly sand blasted, sprayed with isopropyl alcohol and wiped with lint-free cloth. The plastic spacers which are used to fix the location of the bond ends also align the centerlines of the adherends. The adhesive was injected into the joints and allowed to cure at room temperature for one week before the plastic spacers were removed. The process is then repeated for the second joint of the tensile specimens. Note that each compressive specimen has only one joint. Double-jointed specimens are used for the tensile tests to simplify the required test fixture.

### Single-Cycle Tests

The single-cycle specimens were tested in a standard electrohydraulic test frame. Figure 9

shows a compressive specimen between two platens. The tensile specimens were attached to the test frame with eyebolts which were screwed into the threaded ends of the steel adherends. The composite adherend of each specimen was instrumented with three strain gages - equally spaced along the circumference - to assess the uniformity of the loading.

Figure 10 shows the failure loads for the compressive single-cycle tests. All of the compressive specimens failed abruptly when the adhesive completely debonded from the steel adherend. On average, the joints with tapered adherends were 25% stronger than the baseline joints (48280 versus 38410 pounds). Unfortunately, the modified joints also exhibited more scatter than the baseline joints. Still, the differences in the data support the claim that tapering the steel adherend increases the single-cycle compressive strength of these joints.

Figure 11 shows the failure loads for the tensile single-cycle tests. Note that the data come in pairs since each tensile specimen has two joints. Two of the six specimens were comprised of one baseline and one modified joint. The other four specimens had either two baseline or two modified joints. In general, the levels shown for the tensile specimens represent the applied load when the composite adherend failed. The adhesive bond only failed in two of the joints. Both of debonds occurred in joints which had tapered adherends. It should be noted that these debonds occurred at load levels where the failure of the composite adherend was imminent. In one of these joints, the adhesive debonded from the steel adherend. In the other joint, the adhesive debonding probably initiated at the composite adherend interface. As mentioned earlier, there was some concern that tapering the adherend could reduce the tensile strength of these joints and/or change the failure mode. It appears that tapering the steel adherend does cause a minor reduction in the single-cycle tensile strength of these joints. However, the overall performance of the joint (in single-cycle loading) is believed to be enhanced by this modification.

### Low-Cycle Fatigue Tests

The fatigue specimens were tested with the same test frame, fixtures, and instrumentation as the single-cycle specimens. The compressive and tensile specimens remained in compression and

tension, respectively, throughout the tests. The magnitude of the peak load was 10 times the magnitude of the minimum load for all of the specimens. The tests were conducted at approximately 5 Hz. Both joints of the tensile specimens were inspected for debonding throughout the tests. Since a small debonded region on one joint doesn't significantly affect the other joint, each tensile specimen produced two data points.

Figure 12 shows the results of the low-cycle fatigue tests. Each data point (except for the solitary runout) represents the number of cycles a joint withstood for a given loading cycle before the initial adhesive debonding was observed. It should be noted that the adhesive debonded from the steel adherend in all of the compressive specimens and the baseline tensile specimens. However, the adhesive debonded from the composite adherend in the modified tensile specimens. The potential for this change in the failure mode was addressed in the analyses section of this paper. As with the single-cycle tests, both joint designs performed better in tension than compression. Note that tapering the adherend clearly improves the performance of these joints in low-cycle compressive fatigue. For example, at  $10^4$  cycles, the tapered joints can carry roughly 50% more load than the baseline design joints. In addition, the reduction in tensile strength is fairly minor. Thus, the overall performance of this joint is believed to be enhanced (in low-cycle fatigue) by tapering the steel adherend.

A final comment should be made regarding the performance of the modified joint in high-cycle ( $10^6$  and higher) fatigue. Although no data is available for the modified joints, an extrapolation of the existing data suggests that tapering the steel adherend may not provide an advantage in this regime. However, even if the modified and baseline design joints perform similarly in high-cycle fatigue, tapering the steel adherend would still be beneficial for high-cycle fatigue applications which involve infrequent (but detrimental) high-amplitude loads.

### SUMMARY

The durability of adhesively bonded lap joints directly affects the viability of wind turbines that utilize these joints as blade attachments. Previous efforts established that the adhesive peel stresses strongly influence the strength of the composite-to-

steel joints under consideration. In this study, several different tapers (to the steel adherend) were evaluated using finite element analysis before arriving at a design which reduced the adhesive peel stresses in the region where failure initiates. Subsequent single-cycle and low-cycle fatigue tests confirmed that tapering the steel adherend produced a significant increase in the compressive strength of these joints and only a minor decrease in their tensile strengths. These joints are much stronger in tension than compression and failure initiates on the compressive side when they are loaded in bending. Thus, the selected modification improves the overall performance of this joint.

### ACKNOWLEDGMENTS

The test specimens were fabricated by J. Morgan. M. E. Stavig assisted with the axial tests of the joints. This work was performed at Sandia National Laboratories. Sandia is a multiprogram laboratory operated by Sandia Corporation, a Lockheed Martin Company, for the United States Department of Energy under Contract DE-AC04-94AL85000.

### REFERENCES

1. K. E. Metzinger and T. R. Guess, "Single-Cycle and Fatigue Strengths of Adhesively Bonded Lap Joint," 36th AIAA Aerospace Sciences Meeting and Exhibit, Reno, Nevada, January 1998.
2. K. E. Metzinger and T. R. Guess, "The Effect of Peel Stress on the Strength of Adhesively Bonded Joints," 37th AIAA Aerospace Sciences Meeting and Exhibit, Reno, Nevada, January 1999.
3. E. D. Reedy, Jr. and T. R. Guess, "Composite-to-metal tubular lap joints: strength and fatigue resistance," *International Journal of Fracture* 63:351-367, 1993.
4. ABAQUS/Standard, Version 5.8.
5. T. R. Guess, E. D. Reedy, Jr., and M. E. Stavig, "Mechanical Properties of Hysol EA-9394 Structural Adhesive," SAND95-0229, Sandia National Laboratories, Albuquerque, New Mexico, February 1995.
6. MIL-HDBK-5E, June 1987.
7. T. R. Guess, E. D. Reedy, Jr., and A. M. Slavin, "Testing Composite-to-Metal Tubular Lap Joints," *Journal of Composites Technology & Research*, Vol. 17, No. 2, April 1995.

Table 1: Isotropic Material Properties

Material	Elastic Modulus (psi)	Poisson's Ratio	Yield Strength (psi)	Hardening Modulus (psi)
Adhesive	$6.0 \times 10^5$	0.37	$4.0 \times 10^3$	$3.0 \times 10^5$
Steel	$2.9 \times 10^7$	0.32	-	-

Table 2: Orthotropic Material Properties - Composite

$E_r$ (psi)	$E_a$ (psi)	$E_t$ (psi)	$\nu_{ra}$	$\nu_{rt}$	$\nu_{at}$	$G_{ra}$ (psi)	$G_{rt}$ (psi)	$G_{at}$ (psi)
$1.45 \times 10^6$	$3.26 \times 10^6$	$4.06 \times 10^6$	0.10	0.10	0.17	$7.25 \times 10^5$	$7.25 \times 10^5$	$7.25 \times 10^5$

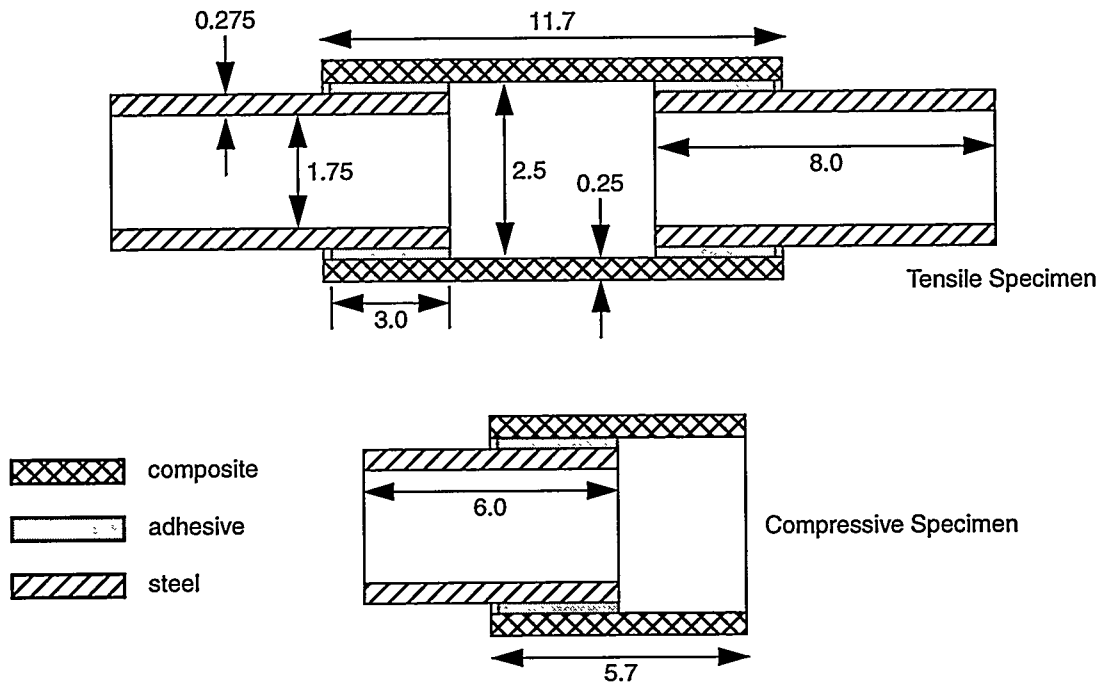


Figure 1. Baseline Joint Geometries (Cut-away View, Dimensions in Inches)

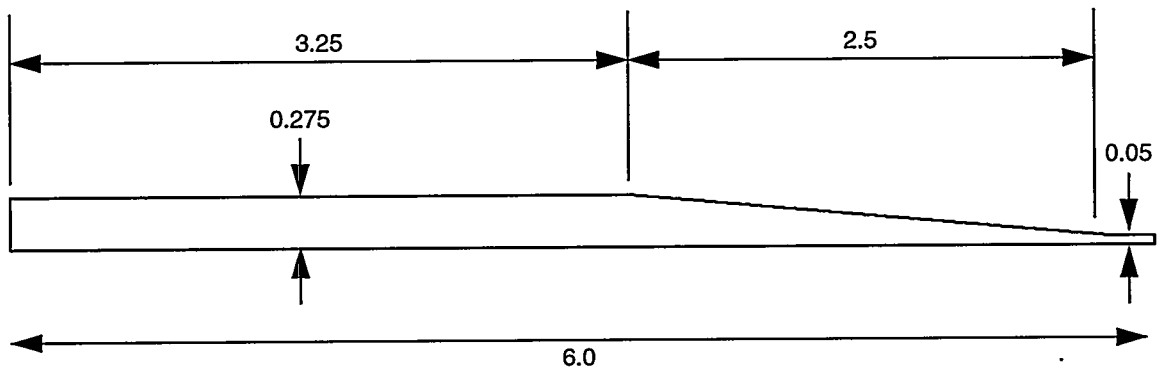


Figure 2. Tapered Adherend Geometry - Compressive Specimen (Cross Section, Dimension in Inches)



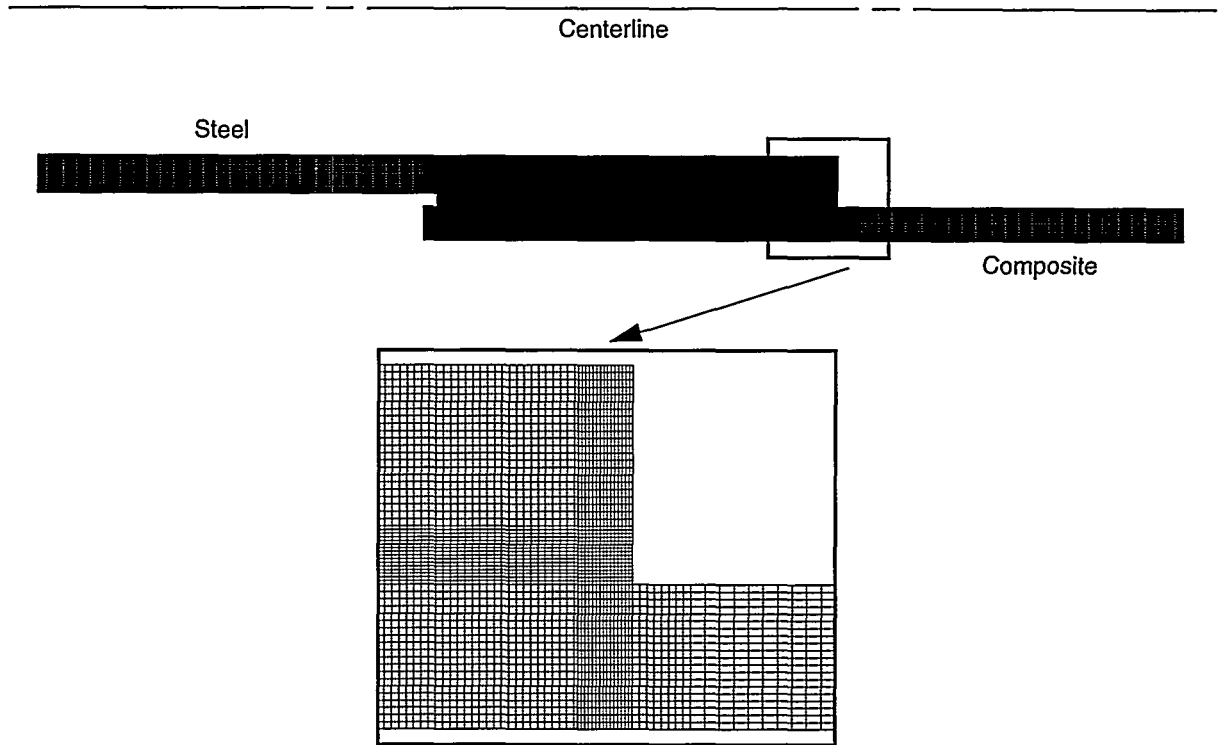


Figure 3. Baseline Joint Finite Element Mesh - Compressive Specimen

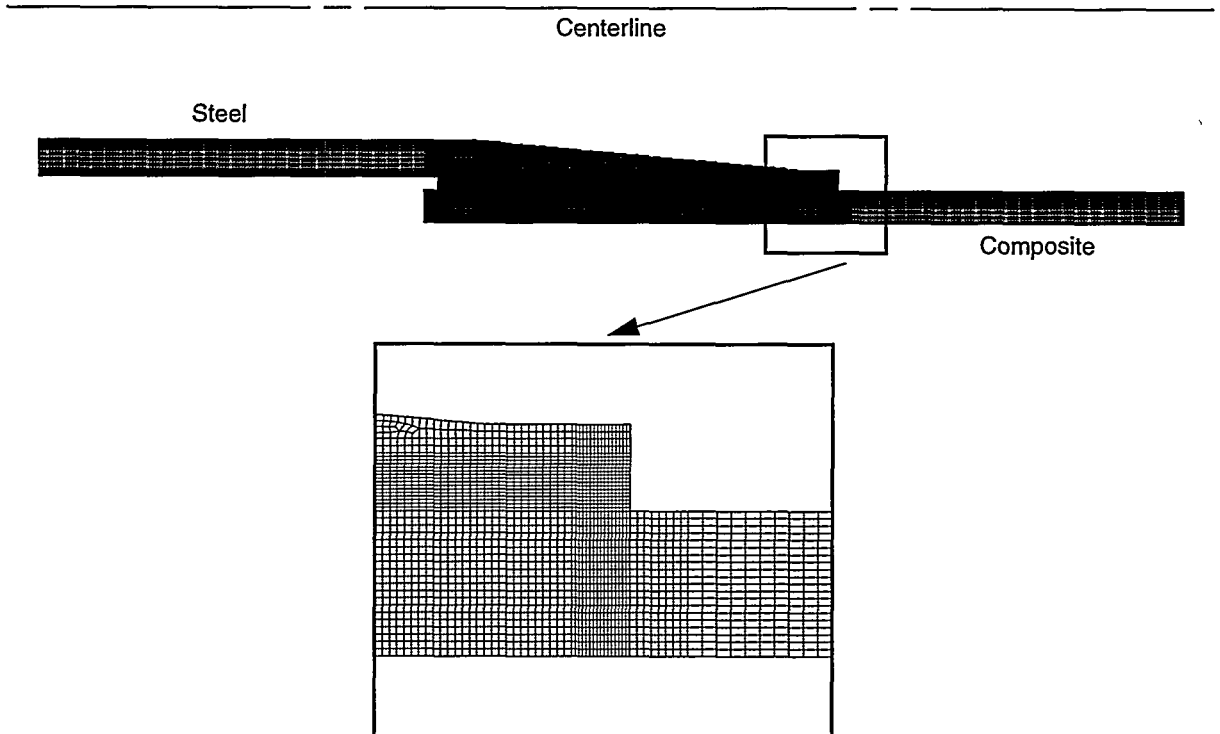


Figure 4. Modified Joint Finite Element Mesh - Compressive Specimen

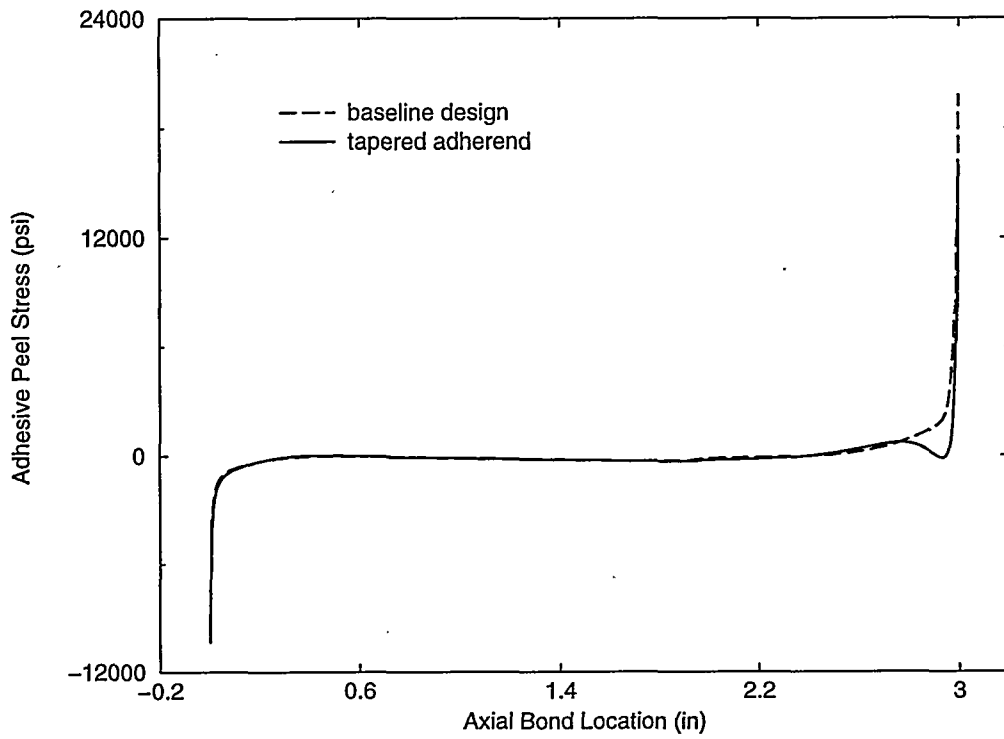


Figure 5. Adhesive Peel Stress at the Steel Adherend Interface - 40000 lb Compressive Load

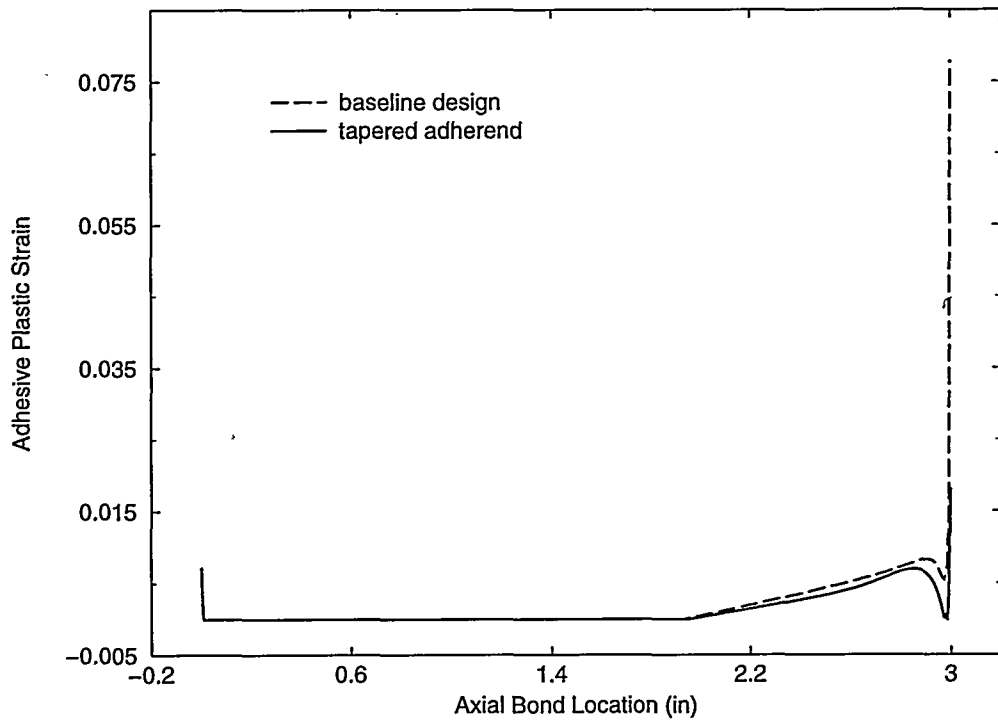


Figure 6. Adhesive Plastic Strain at the Steel Adherend Interface - 40000 lb Compressive Load

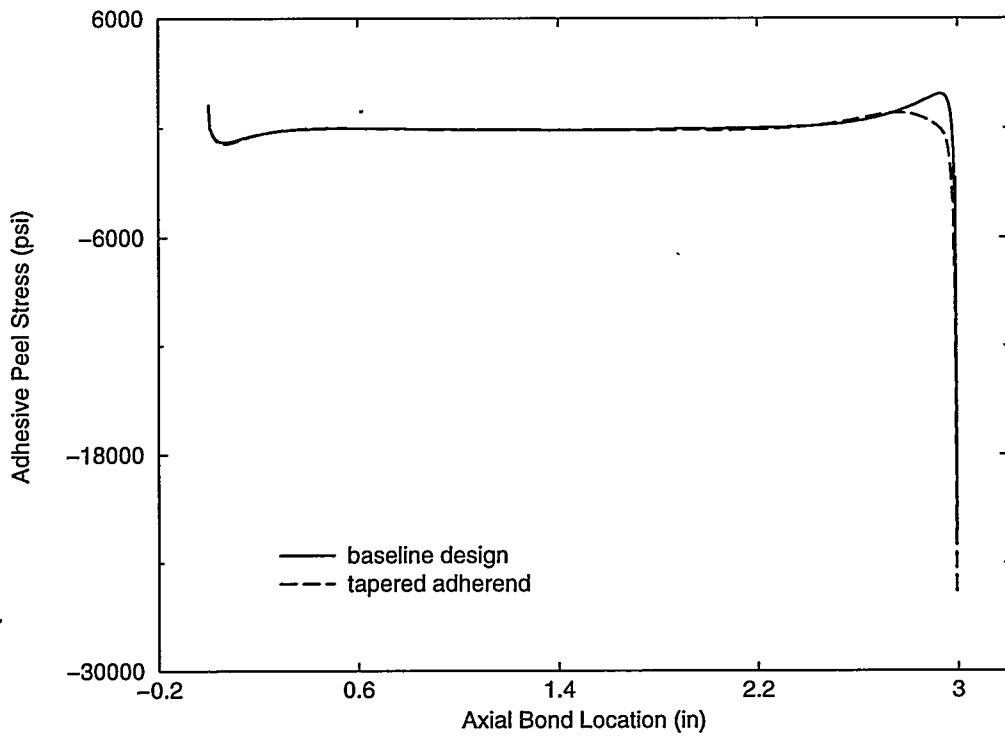


Figure 7. Adhesive Peel Stress at the Composite Adherend Interface - 40000 lb Compressive Load

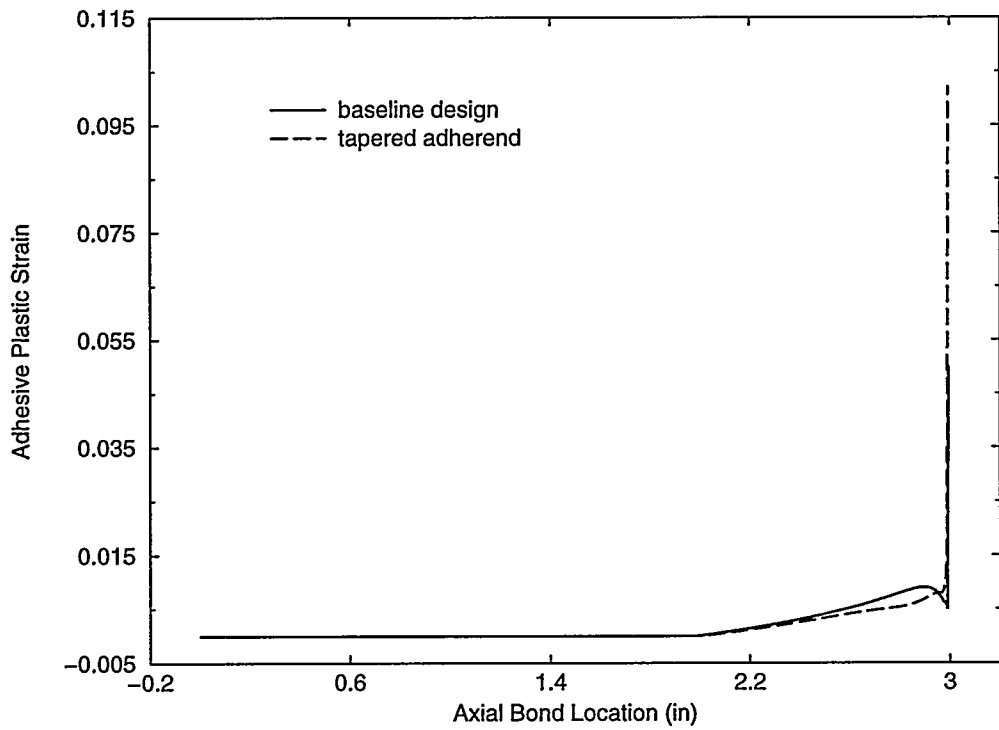


Figure 8. Adhesive Plastic Strain at the Composite Adherend Interface - 40000 lb Compressive Load

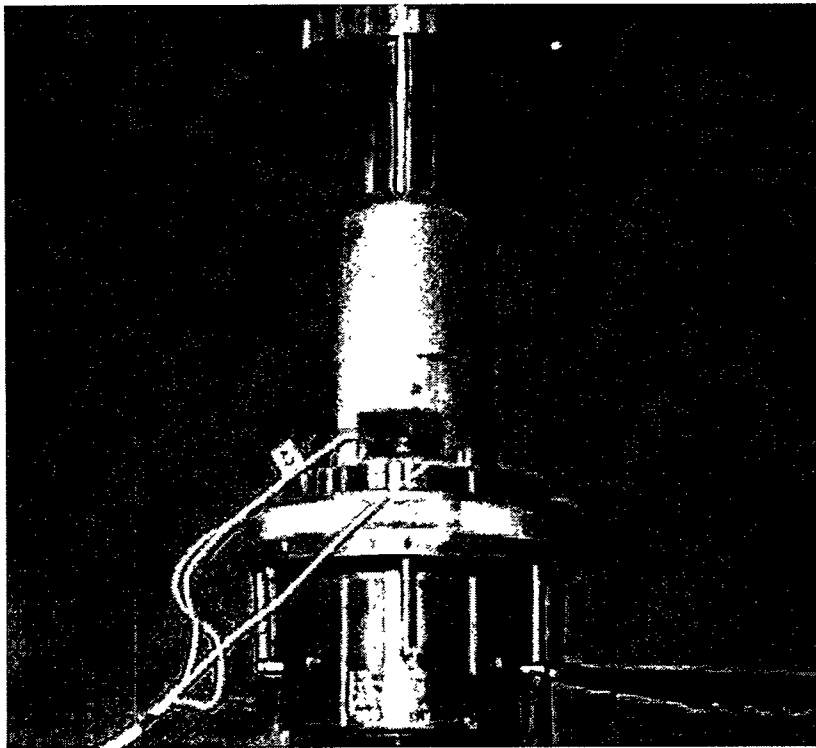


Figure 9. Test Setup (Compressive Specimen)

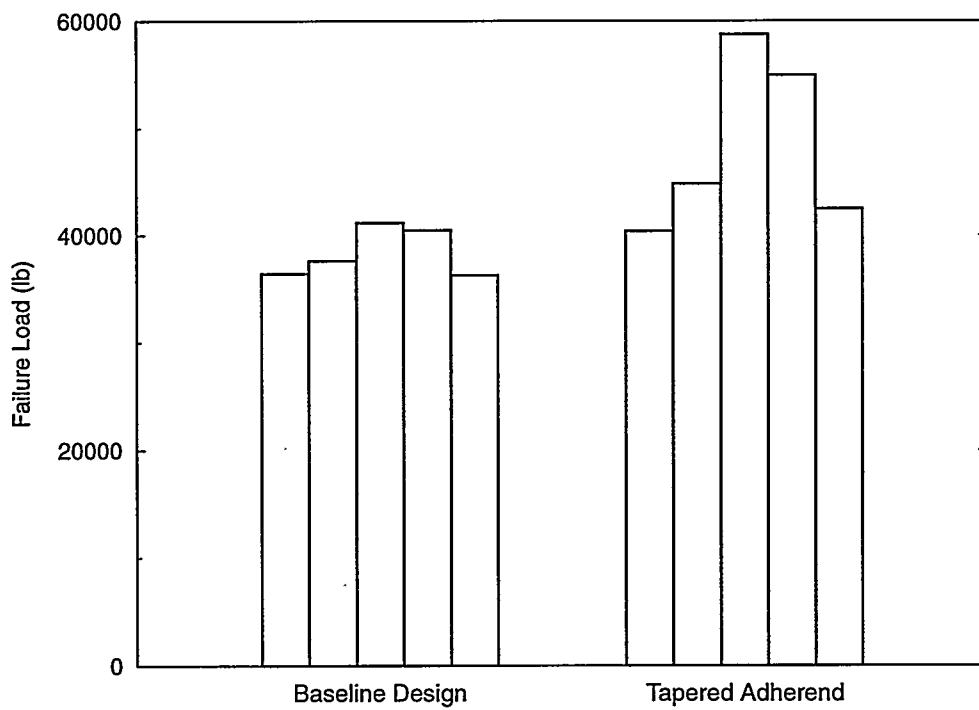


Figure 10. Single-Cycle Compressive Test Results

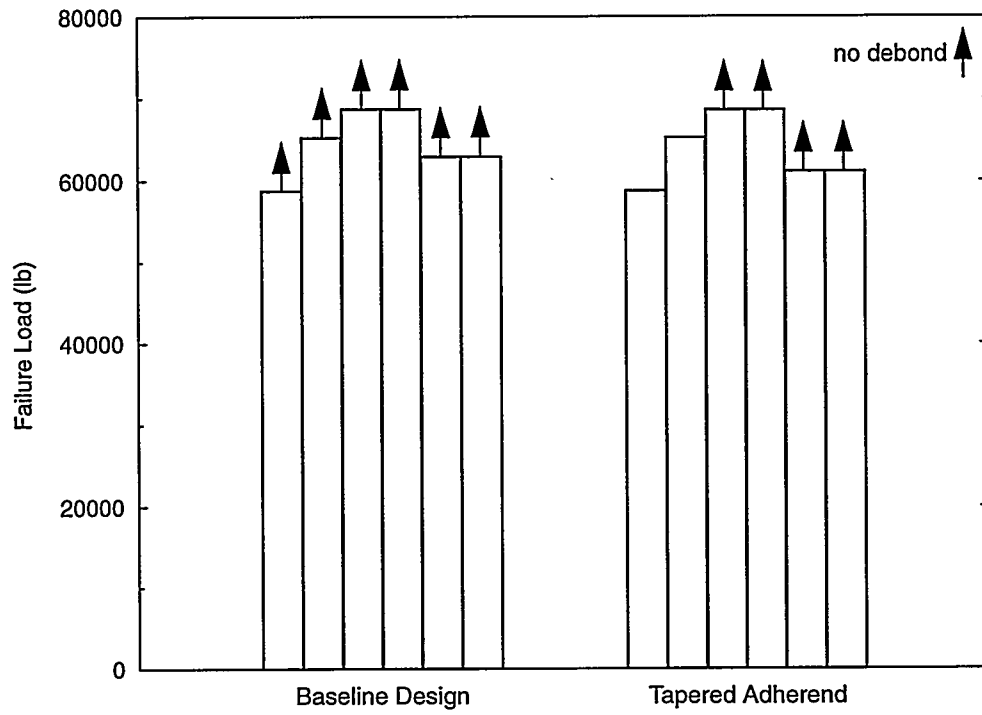


Figure 11. Single-Cycle Tensile Test Results

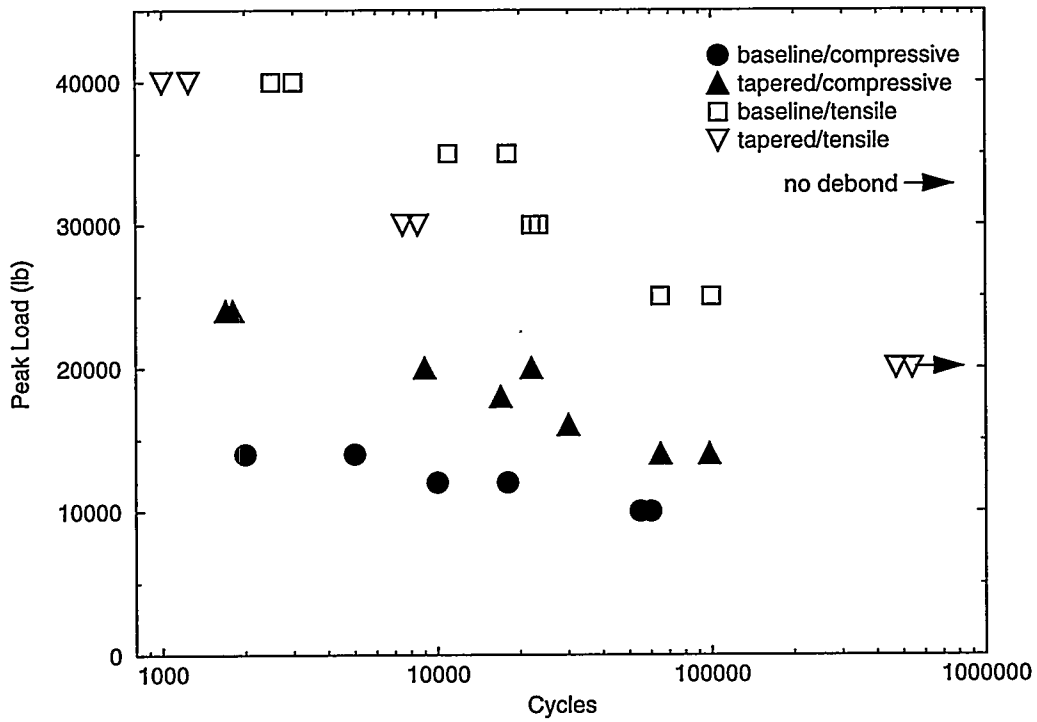


Figure 12. Low-Cycle Fatigue Test Results